



저작자표시-비영리-변경금지 2.0 대한민국

이용자는 아래의 조건을 따르는 경우에 한하여 자유롭게

- 이 저작물을 복제, 배포, 전송, 전시, 공연 및 방송할 수 있습니다.

다음과 같은 조건을 따라야 합니다:



저작자표시. 귀하는 원저작자를 표시하여야 합니다.



비영리. 귀하는 이 저작물을 영리 목적으로 이용할 수 없습니다.



변경금지. 귀하는 이 저작물을 개작, 변형 또는 가공할 수 없습니다.

- 귀하는, 이 저작물의 재이용이나 배포의 경우, 이 저작물에 적용된 이용허락조건을 명확하게 나타내어야 합니다.
- 저작권자로부터 별도의 허가를 받으면 이러한 조건들은 적용되지 않습니다.

저작권법에 따른 이용자의 권리는 위의 내용에 의하여 영향을 받지 않습니다.

이것은 [이용허락규약\(Legal Code\)](#)을 이해하기 쉽게 요약한 것입니다.

[Disclaimer](#)

A Master's Thesis

**Phenylacetaldehyde, a volatile flavor and aroma
compound, inhibits breast cancer stem cells through
the blockade of Stat3/IL-6 signaling pathway**

Ji-Young Kang

**Interdisciplinary Graduate Program in
Advanced Convergence Technology & Science**

**Graduate School
Jeju National University**

February, 2017

A Master's Thesis

**Phenylacetaldehyde, a volatile flavor and aroma
compound, inhibits breast cancer stem cells through
the blockade of Stat3/IL-6 signaling pathway**

Ji-Young Kang

(Supervised by Professor Dong-Sun Lee)

**Interdisciplinary Graduate Program in
Advanced Convergence Technology & Science**

**Graduate School
Jeju National University**

February, 2017

휘발성 향기 물질 phenylacetaldehyde의 Stat3/IL-6
경로 차단을 통한 유방암 줄기세포 억제 효과




지도교수 이 동선

강 지영

이 논문을 이학 석사학위 논문으로 제출함

2016 년 12 월

강지영의 이학 석사학위 논문을 인준함

심사위원장 서 동 기 
위 원 김 소 미 
위 원 이 동 선 

제주대학교 대학원

2016 년 12 월

**Phenylacetaldehyde, a volatile flavor and aroma
compound, inhibits breast cancer stem cells through
the blockade of Stat3/IL-6 signaling pathway**

Ji-Young Kang

(Supervised by Professor Dong-Sun Lee)

**A thesis submitted in partial fulfillment of the requirement of the
degree of Master of Science**

2016. 12

This thesis has been examined and approved.

Dong Sun Lee

Somi Kim Cho

Dong Sun Lee

2016.12

Graduate School

Jeju National University



CONTENTS

CONTENTS	i
LIST OF FIGURES	ii
ABSTRACT	iii
1. Introduction	1
2. Materials and Methods	3
3. Results	8
3.1. PAA inhibits multiple cancer hallmarks in breast cancer cells.	8
3.2. PAA suppresses growth of breast tumors <i>in vivo</i>	11
3.3. PAA treatment inhibits breast CSCs.	13
3.4. PAA reduced the percentage of CD44 ^{high} /CD24 ^{low} and ALDH ⁺ breast cancer cells.	15
3.5. PAA decreased self-renewal gene expression in breast CSCs and proliferation of mammospheres.	17
3.6. PAA inhibits the Stat3 signaling pathway and IL-6 secretion in breast CSCs. .	19
4. Discussion	22
References	24

LIST OF FIGURES

Figure 1. Effect of PAA on the various cancer hallmarks in breast cancer cells.	9
Figure 2. Inhibitory effect of PAA on breast tumor growth in a xenograft model.	12
Figure 3. Effect of PAA on mammosphere formation.	14
Figure 4. Effect of PAA on expression of breast CSC markers.	16
Figure 5. Effect of PAA on sustenance of breast CSCs.	18
Figure 6. The effects of PAA on the Stat3 signaling pathway and IL-6 secretion in MCF-7 mammospheres.	20

Abstract

Breast cancer is the most common cancer in the world and a major leading cause of cancer deaths in women. Although the availability of diverse effective therapies has improved survival rates, treating breast cancer is still considerable challenges due to the existence of CSCs. CSCs represent capable of treatment resistance, disease recurrence, and metastasis. In this study, we evaluated the PAA, a flavor and aroma volatile compound, for its efficacy to inhibit breast CSCs. Our results showed that PAA treatment significantly inhibited breast cancer cell proliferation, migration and colony formation. In addition, PAA induced the apoptosis of breast cancer cells and suppressed tumor growth *in vivo*. PAA reduced the mammosphere forming ability of breast cancer cells, the CD44^{high}/CD24^{low} subpopulation and the percentage of ALDH+ cells. PAA also decreased the expression of self-renewal genes including Nanog, Sox2, Oct4 and CD44 as well as induced ROS activity. Furthermore, PAA blocked the Stat3 signaling pathway via inhibition of nuclear Stat3 phosphorylation and IL-6 secretion. Taken together, our findings suggest that PAA has anti-cancer and anti-CSC activities in breast cancer cells. This study provides evidence that PAA may improve the limited effects of breast cancer therapy.

1. Introduction

Worldwide, breast cancer is one of the most frequently diagnosed cancer and is responsible for more than 522,000 deaths of women annually [1]. Despite early detection and improvements in the diverse therapies, breast cancer is still a fatal disease because of resistance to therapy, metastasis and recurrence. The common cause of these problems is attributed to the presence of cancer stem cells (CSCs) [2, 3]. CSCs are a highly tumorigenic cell type that exist as a small population within the tumor mass [4]. CSCs were identified first from acute myeloid leukemia (AML) [5] and then from many types of solid tumors, including breast, brain, colon, pancreatic, lung, prostate and ovarian cancers [6]. CSCs are typically identified based on biochemical properties such as aldehyde dehydrogenase-1 (ALDH1) activity or expression of specific cell surface marker [7-9]. In addition, CSCs express specific genes, including Nanog, Sox2, Oct4, and CD44 [10]. Multiple signaling pathways containing Wnt/ β -catenin, TGF- β , STAT3, NF- κ B, Hedgehog and Notch plays an important role in maintaining the CSCs through continuous self-renewal and differentiation [11-14]. A cytokine network such as interleukin (IL)-6 and IL-8 also regulated CSCs self-renewal [15]. Moreover, oxidative stress caused by accumulation of reactive oxygen species (ROS) influences the self-renewal ability of stem cells in cancer [16]. CSCs are able to self-renewal and contribute to tumor resistance/relapse [17], therefore, therapeutics specifically targeting CSCs may provide an effective strategy to overcome cancer.

Signal transducers and activators of transcription 3 (Stat3) is known to regulate CSC proliferation and self-renewal. Stat3 is activated by members of the Jak/Tyk kinases family in response to various kinds of cytokines and growth factors. Upon activation, Stat3 undergoes phosphorylation, homodimerization, nuclear translocation, and DNA binding, which subsequently leads to transcription of various target genes [18, 19]. IL-6, a major

mediator of the inflammatory response, has been shown to be a regulator of breast CSCs self-renewal through activation of Stat3. Secreted IL-6 activates Stat3 and promotes tumorigenicity, angiogenesis, and metastasis [20, 21]. The IL-6/Jak1/2/Stat3 signaling pathway plays an important role in the conversion of non-stem cancer cells (NSCCs) into CSCs and it also helps in self-renewal of CSCs [22].

Phenylacetaldehyde (PAA) is important for the aroma and flavor of many foods, such as tomato. PAA is also a major contributor to an insect-attracting scent in many flowers, particularly roses [23]. In the present study, we investigated a novel effect of PAA on breast cancer therapy by targeting CSCs. We provide evidence that PAA effectively inhibited the various hallmark associated properties of breast CSCs and *in vivo* tumor growth. Therefore, our findings indicate that PAA is a promising candidate as breast CSCs inhibitor.

2. Materials and Methods

2.1. Cell lines and reagents

Human breast cancer cell lines MCF-7 and MDA-MB-231 were obtained from the American Type Culture Collection (ATCC; Manassas, VA, USA). MCF-7 cell was grown in RPMI-1640 (HyClone, Logan, UT, USA) supplemented with 10% fetal bovine serum (FBS; HyClone), 100 U/ml penicillin (HyClone), and 100 µg/ml streptomycin (HyClone). MDA-MB-231 cell was grown in DMEM (HyClone) supplemented with 10% FBS, 100 U/ml penicillin, and 100 µg/ml streptomycin. The cell lines were maintained at 37°C in a humidified incubator with 5% CO₂.

Phenylacetaldehyde and doxorubicin were purchased from Sigma-Aldrich Co. (St. Louis, Mo, USA).

2.2. Mammosphere formation assay

The mammospheres (CSCs) were cultured in MammoCult™ medium (StemCell Technologies, Vancouver, BC, Canada), with 4 µg/ml heparin, 0.48 µg/ml hydrocortisone, 100 U/ml penicillin, and 100 µg/ml streptomycin. MCF-7 and MDA-MB-231 were seeded in ultra-low attachment 6-well plates (Corning, Tewksbury, MA, USA) at a density of 3.5-4.0×10⁴ and 0.5-1.0×10⁴ cells per well in stem cell medium. On the 7th day, the plate was scanned under the Umax scanner and the number of mammospheres was counted with an automated counting program called NIST's Intergrated Colony Enumerator (NICE) [24].

2.3. Cell proliferation assay

MCF-7 and MDA-MB-231 were seeded in 96-well microplates at a density of 1×10⁶ cells per plate. Cells were treated with increasing concentrations of PAA as indicated. After 48 h of incubation, cell viability was assessed by A CellTiter 96® AQueous One Solution Cell

Proliferation Assay kit (Promega, Wisconsin, USA) according to the manufacturer's instruction. The visible absorbance at 490 nm of each well was quantified using a microplate reader (Dynex Revelation, Dynex Ltd., Billingshurst, UK). All results were assessed in triplicate.

2.4. Caspase 3/7 activity assay

Caspase 3/7 activity was measured using the manufacturer's protocol of Caspase-Glo[®] 3/7 Assay Kit (Promega, Wisconsin, USA). After treatment with different concentrations of PAA, the caspase 3/7 reagent was added to 96-well plates. Following incubation at room temperature for 1 h, caspase 3/7 activity was determined from the fluorescence measured using a GloMax[®] Explorer Luminometer (Promega, Wisconsin, USA).

2.5. Annexin V-FITC/PI analysis

MDA-MB-231 cells were seeded in 6-well plates and treated with 0.2 mM PAA for 24 h. The percentage of cells undergoing apoptosis was detected using a FITC Annexin V Apoptosis Detection Kit II (BD, San Diego, CA, USA) and flow cytometry (Accuri C6, BD, San Diego, CA, USA).

2.6. Hoechst staining assay

MDA-MB-231 cells were treated with 0.2 mM PAA for 24 h. After treatment, cells were incubated with Hoechst 33342 (10 mg/ml) at room temperature for 20 min and washed with PBS. Changes in nuclear morphology were detected by fluorescence microscopy (Nikon, Tokyo, Japan).

2.7. Wound-healing assay

For detection of cell migration, MDA-MB-231 cells were seeded into a 6-well plate until 90%

confluent. A wound was made using a sterile white micropipette tip and then cells were treated with PAA. The plates were photographed at 0 and 18 h to monitor the migration of cells in the wounded area.

2.8. Clonogenic assay

MDA-MB-231 cells (1×10^3 cells/well) were seeded into a 6-well plate and treated with different concentrations of PAA. After 24 h, the media was replaced with fresh media and cultured for 7 to 10 days, to let the visible cells propagate to sizable colonies for quantification. Then, the colonies were washed twice with PBS, fixed with methanol-acetic acid at 3:1 ratio, and stained with 0.04% crystal violet for 30 min at room temperature. The number of colonies formed in plate was counted after scanning images by the Umax scanner.

2.9. Flow cytometry

FACS analysis was performed using Accuri C6 (BD, San Diego, CA, USA). CD24 and CD44 expression of MDA-MB-231 cells were examined by FACS analysis using anti-CD44-FITC and anti-CD24-PE antibodies (BD pharmingen, San Diego, CA, USA). The ALDEFLUOR kit (STEMCELL Technologies Inc., Vancouver, BC, Canada) was used to isolate cell populations with high ALDH enzymatic activity in MCF-7. Cells were incubated with a fluorescent ALDH substrate, BODIPY-aminoacetaldehyde (BAAA), for 45 min at 37°C. As a negative control, we treated with 50 μ M diethylaminobenzaldehyde (DEAB), an ALDH-specific inhibitor. Flow cytometry was used to sort ALDH-positive and negative cells.

2.10. Animal experiments

NOD-SCID (BALB/cSlc (nu/nu)) female nude mice were divided into 4 groups (6 mice/group). The 6 mice were received no treatment as a negative control. Another 6 mice was given a mammary pad injection of PAA (10-50 mg/kg) and the other 6 mice were injected doxorubicin as a positive control. The last group was used as non-tumor group

without treatment. The tumor volumes were measured twice per week and then calculated using the formula $(\text{length} \times \text{width}^2)/2$.

2.11. Real-time PCR

Total RNA was extracted using the TaKaRa MiniBEST Universal RNA extraction Kit (TaKaRa, Tokyo, Japan). Gene expression levels in all samples were examined using the TOPreal™ One-step RT qPCR Kit (Enzynomics, Daejeon, Korea) according to the manufacturer's protocol. Real-time PCR was performed using the Thermal Cycler Dice Real Time System (TaKaRa, Tokyo, Japan). The primer sequences used were: NANOG-F, 5'-ATGCCTCACACGGAGACTGT-3' and R, 5'-AAGTGGGTTGTTTGCCTTTG-3'; SOX2-F, 5'-TTGCTGCCTCTTTAAGACTAGGA-3' and R, 5'-CTGGGGCTCAAACCTTCTCTC-3'; OCT4-F, 5'-AGCAAACCCGGAGGAGT-3' and R, 5'-CCACATCGGCCTGTGTATATC-3'; CD44-F, 5'-AGAAGGTGTGGGCAGAAGAA-3' and R, 5'-AAATGCACCATTTCCTGAGA-3'; β -actin-F, 5'-TGTTACCAACTGGGACGACA-3' and R, 5'-GGGGTGTGTAAGGTCTCAAA-3'. Relative mRNA expression of target genes was normalized to β -actin and calculated using the comparative CT method.

2.12. Measurement of ROS levels

MDA-MB-231 cells were seeded in 96-well white plates and treated with 0.2 mM PAA. After 24 h, ROS activity was detected by a ROS-Glo™ H₂O₂ Assay Kit (Promega, Wisconsin, USA) following the manufacturer's instructions. ROS-Glo™ detection solution was added to each well and incubated for 20 min. Then, luminescence intensity was quantified using a GloMax® Explorer Luminometer (Promega, Wisconsin, USA).

2.13. Western blot analysis

The concentration of proteins extracted from MCF-7 mammospheres treated with 0.4 mM PAA was determined with Pierce BCA Protein Assay Kit (Thermo Fisher Scientific, IL,

USA). Equal amounts of protein were separated on a 10% SDS-PAGE and transferred to PVDF membranes. After blocking with 5% nonfat dry milk in PBS-Tween 20 (0.1%, v/v) for 1 h, the membranes were incubated overnight at 4°C with the following primary antibodies: Stat-3, p65 and phospho-Stat3 (Cell Signaling, Beverly, MA, USA). Lamin B was used as a loading control in nuclear extracts. Further incubation with appropriate horseradish peroxidase-conjugated secondary antibodies, blotted proteins were detected using the enhanced chemiluminescence kit (Santa Cruz Biotechnology Inc., Dallas, TX, USA).

2.14. Electrophoretic mobility shift assay

Electrophoretic mobility shift assay (EMSA) was done using a LightShift Chemiluminescent EMSA Kit (Thermo Fisher Scientific, IL, USA) according to the manufacturer's instructions. Nuclear extracts were prepared from MCF-7 mammospheres and synthetic complementary oligonucleotides were annealed. The sequence of the oligonucleotides for Stat3 were: 5'-CTTCATTTCCCGGAAATCCCTA-Biotin3' and 5'-TAGGGATTTCCGGGAAATGAAG-Biotin3'. The binding reaction was carried out at room temperature for 20 min, using biotin-end-labeled target DNA and nuclear extracts. Products were loaded onto native 6% polyacrylamide gel and transferred onto a nylon membrane at 100 V for 30 min. Transferred DNA was cross-linked to the membrane for 15 min and detected using a Chemiluminescent Nucleic Acid Detection Module Kit (Thermo Fisher Scientific, IL, USA).

2.15. Statistical analysis

All data in this study were analyzed by GraphPad Prism 5.0 (GraphPad Software, San Diego, CA, USA) and expressed as the mean \pm SD. Statistical analysis was performed using a Student's test. A p-value < 0.05 was considered to indicate statistical significance.

3. Results

3.1. PAA inhibits multiple cancer hallmarks in breast cancer cells.

We first examined the effect of PAA on various cancer hallmark capabilities (proliferation, apoptosis, migration and colony formation) in breast cancer cells. MTS assay was used to determine the anti-proliferative effect of PAA in two human breast cancer cell lines, MCF-7 and MDA-MB-231. As shown Fig. 1B and C, PAA showed anti-breast cancer activity in both cell lines in a dose-dependent manner. To examine whether PAA treatment induce apoptosis, we analyzed apoptosis by Annexin V/PI staining, an indicator of apoptosis. We showed that PAA induced the percentage of apoptotic cells (Fig. 1D). Additionally, we observed that PAA treatment induced the activation of caspase 3/7 (Fig. 1E) and changed the morphology of cells (Fig. 1F). We further checked effect of PAA on migration and colony forming potential of MDA-MB-231 cells. PAA treatment significantly reduced cell migration and colony formation in dose-dependent manner (Fig. 1G and H). Collectively, these results showed that PAA effectively inhibits the various cancer hallmarks.

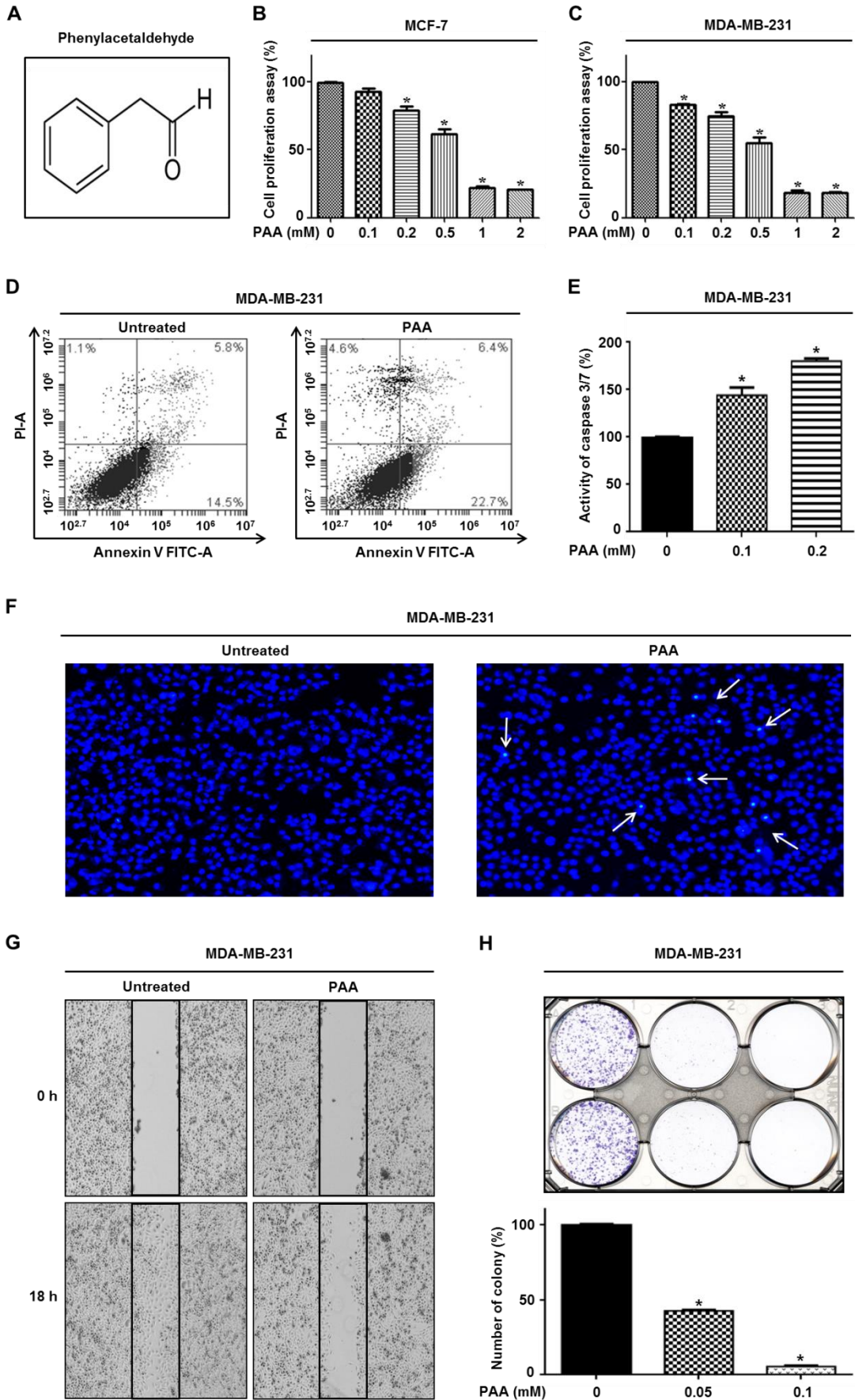


Figure 1. Effect of PAA on the various cancer hallmarks in breast cancer cells. (A) The chemical structure of phenylacetaldehyde (PAA). (B and C) MCF-7 and MDA-MB-231 cells were treated with 0, 0.1, 0.2, 0.5, 1 and 2 mM of PAA. After 48 h of incubation, the anti-proliferation effect of PAA was assessed by MTS assay. (D) The rates of cell apoptosis were increased by PAA treatment. The lower-right quadrant of each plot indicates early apoptotic cells and the upper-right quadrant indicates late apoptotic cells. (E) Caspase 3/7 activity in MDA-MB-231 cells following treatment with PAA for 24 h. (F) Morphology of apoptotic cell nuclei was observed by Hoechst 33342 staining using a fluorescence microscope (magnification, $\times 200$). (G) Wound-healing assay was performed to evaluate the migration potential. Images were captured at time 0 and 18 h after wounding. (H) Colonies were counted and calculated as a relative percentage of the untreated cells. The data represent the mean \pm SD of three independent experiments. * $p < 0.05$.

3.2. PAA suppresses growth of breast tumors *in vivo*.

To confirm the *in vivo* effect of PAA in tumorigenesis, we injected MDA-MB-231 cells into the female nude mice. We observed that PAA-treated group significantly decreased tumor growth compared with other groups (Fig. 2A). The tumor volume of PAA-treated group was smaller than the control group (Fig. 2B). Moreover, the tumor weight of PAA-treated group was less than the control group (Fig. 2C). No considerable change in body weight of the mice was observed. Our results suggest that PAA significantly suppressed breast tumor growth in the xenograft model.

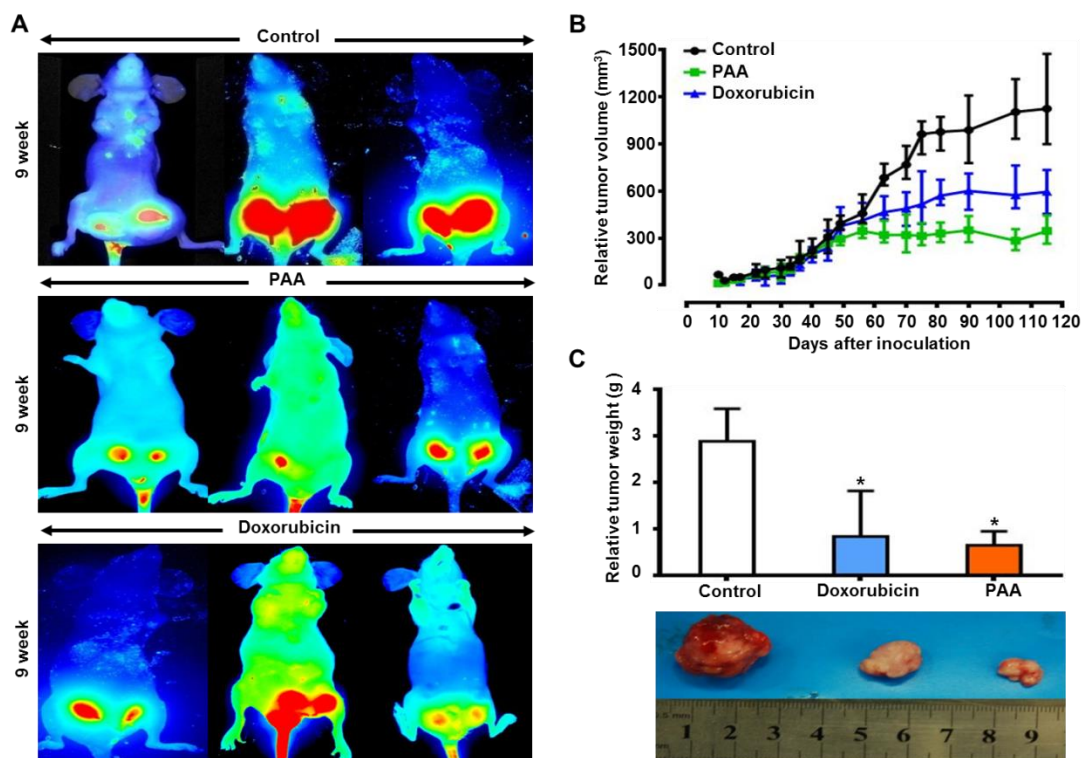


Figure 2. Inhibitory effect of PAA on breast tumor growth in a xenograft model. MDA-MB-231 cells (3×10^7 cells/mouse) were injected into the mammary fat pad of each immunodeficient NOD-SCID female nude mouse. (A) Images were captured with the Odyssey[®] Imager (LICOR, Pearl imaging systems, USA). The high grade of tumors using the IRDye 800 CW optical probe (2DG) was used to detect breast tumors in the 800 nm channel, represented in pseudo-color. (B) Tumor growth was monitored during the experimental period by measuring the length and width with caliper. Tumor volume was calculated as $(\text{length} \times \text{width}^2)/2$. (C) At the end of therapy, the mice were sacrificed and the tumors were extracted. The final tumor weight and size are shown in the upper and lower panel, respectively. * $p < 0.05$ when compared with control.

3.3. PAA treatment inhibits breast CSCs.

Next, we treated with different concentration of PAA to the primary mammospheres derived from MCF-7 and MDA-MB-231 cells to investigate whether PAA treatment would inhibit mammosphere formation of both cell lines. The results showed that the size and number of MCF-7 mammospheres were decreased by 50% to 90% (Fig. 3A). MDA-MB-231 mammospheres were also reduced in a dose-dependent manner (Fig. 3B).

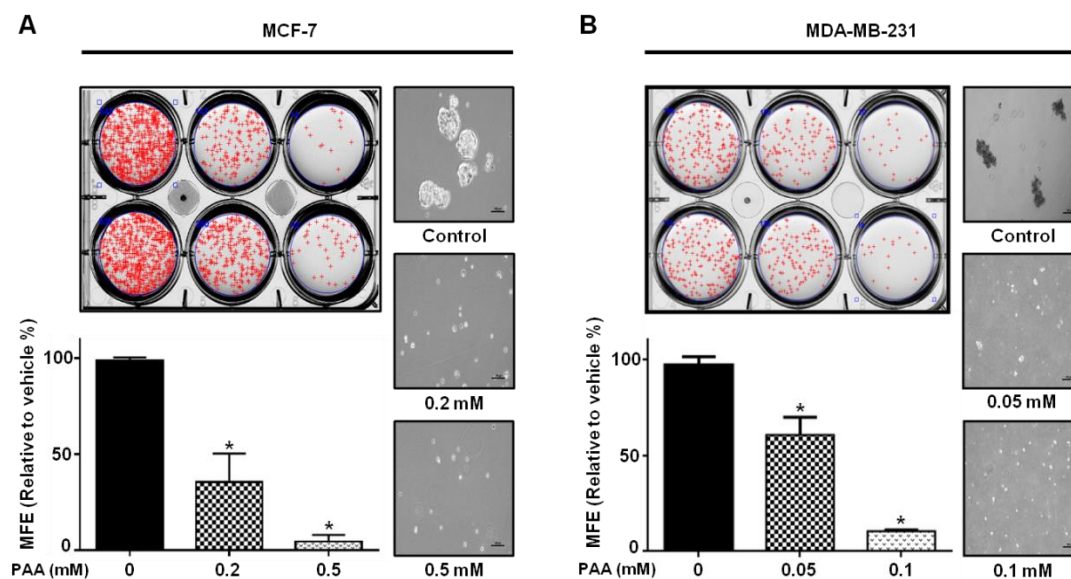


Figure 3. Effect of PAA on mammosphere formation. (A-B) MCF-7 and MDA-MB-231 cells were cultured in mammosphere-forming conditions and incubated with PAA. After 7 days, PAA treatment reduced the formation of mammospheres derived from MCF-7 (A) and MDA-MB-231 cells (B). Images were obtained at $\times 10$ magnification. Scale bar represents 100 μm .

3.4. PAA reduces the percentage of CD44^{high}/CD24^{low} and ALDH+ breast cancer cells.

To determine the effect of PAA as a CSCs inhibitor, we assessed the expression of CD44^{high}/CD24^{low} reported breast CSC markers. As shown Fig. 4A, the proportion of CD44^{high}/CD24^{low} in MDA-MB-231 cells were decreased by 50% significantly after the treatment. Additionally, we performed the Aldefluor assay which measures expression of ALDH+ cells, for ALDH+ cells are enriched in CSCs. Our data showed that PAA reduced the ALDH+ cells from 0.9% to 0.1% (Fig. 4B).

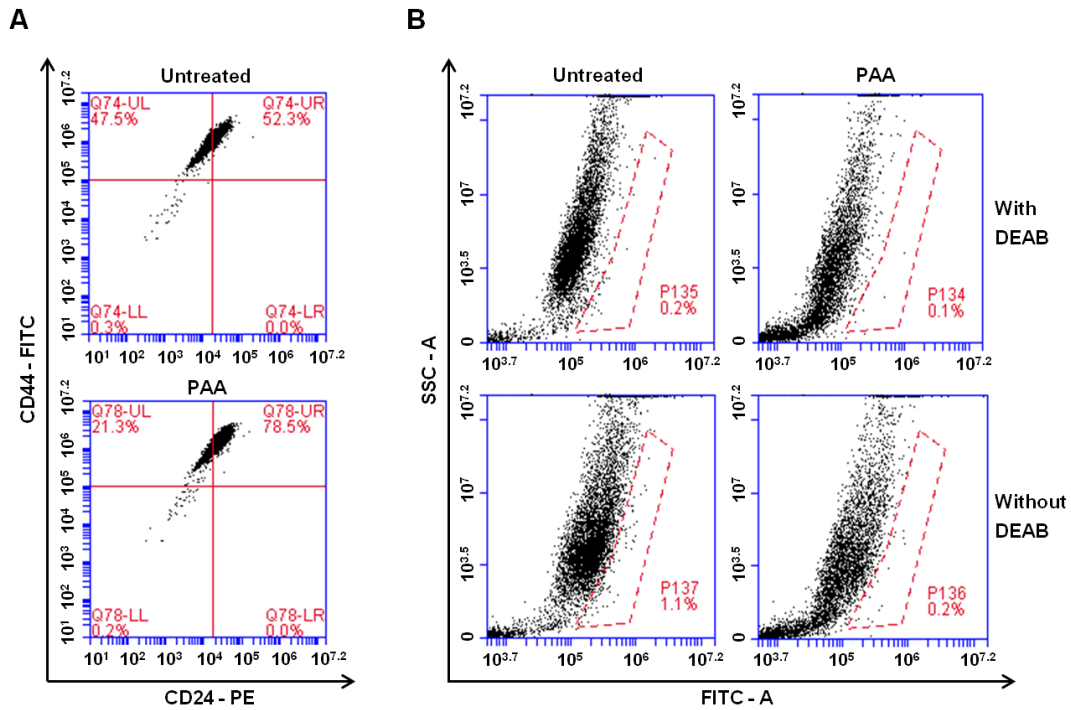


Figure 4. Effect of PAA on expression of breast CSC markers. (A) Flow cytometry analysis of CD44^{high}/CD24^{low} population in MDA-MB-231 cells treated with 0.4 mM PAA. Quadrant 2 indicates CD44^{high}/CD24^{low} cells. (B) A set of representative flow cytometry dot plots of Aldefluor assay with or without DEAB. MCF-7 cells were treated with 0.4 mM PAA for 24 h and the percentage of ALDH⁺ cells were measured through flow cytometry. The region of ALDH⁺ cells was gated in the box.

3.5. PAA decreases self-renewal gene expression in breast CSCs and proliferation of mammospheres.

We used real-time PCR to evaluate the ability of PAA to decrease the expression of self-renewal genes. As a result, the expression levels of self-renewal genes including Nanog, Sox2, Oct4 and CD44 were diminished by the treatment (Fig. 5A). We also examined the levels of ROS after PAA treatment since ROS activity is associated with CSCs. Generally, increased ROS have been shown to kill CSCs. In contrast, low levels of ROS are related in the stemness of CSCs [25]. Our results showed that PAA significantly induced ROS activity in MDA-MB-231 cells (Fig. 5B). Moreover, we treated with PAA in mammospheres derived from MCF-7 cells and observed that PAA effectively inhibited mammosphere proliferation (Fig. 5C).

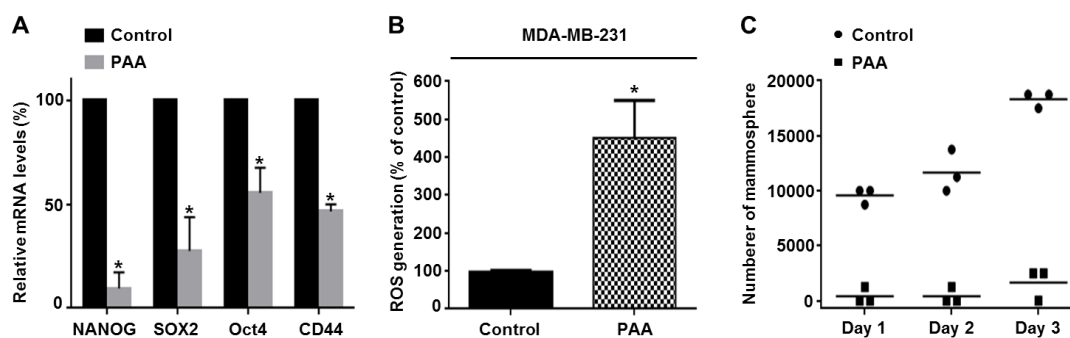


Figure 5. Effect of PAA on sustenance of breast CSCs. (A) The mRNA expression of indicated self-renewal genes in MCF-7 mammospheres treated with 0.4 mM PAA determined by real-time PCR. β -actin was used as a internal control. (B) ROS levels were measured using ROS-GloTM H₂O₂ Assay Kit. (C) MCF-7 mammospheres treated with 0.4 mM PAA for 2 days were dissociated into single cells and plated in 6-cm dish with an equal number of cells. After 1, 2 and 3days, cells were counted in triplicate and plotted as the mean value. The data represent the mean \pm SD of three independent experiments. * $p < 0.05$.

3.6. PAA inhibits the Stat3 signaling pathway and IL-6 secretion in breast CSCs.

We further investigated the mechanisms that may contribute to the effects of PAA on breast CSCs. Because the Stat3 and NF- κ B signaling pathways are important regulator of CSCs self-renewal, we examined these pathways in mammospheres derived from MCF-7 cells treated with PAA using western blot analysis. The results showed that PAA decreased the phosphorylation of nuclear Stat3 protein. However, the protein levels of nuclear p65 did not reduced after the treatment (Fig. 6A). In addition, we confirmed whether PAA suppressed DNA-binding activity of Stat3 by EMSA assay and showed that DNA-binding ability of Stat3 was inhibited by PAA (Fig. 6B). Together, our findings indicated that PAA inhibits self-renewal of CSCs by targeting Stat3 signaling pathway. Secreted IL-6 is an important survival factor of CSCs [20]. Thus, we measured production of secreted IL-6 by western blot analysis of the mammosphere culture broth using IL-6 antibody. Result in Fig. 6C showed that PAA treatment reduced the production of secreted IL-6.

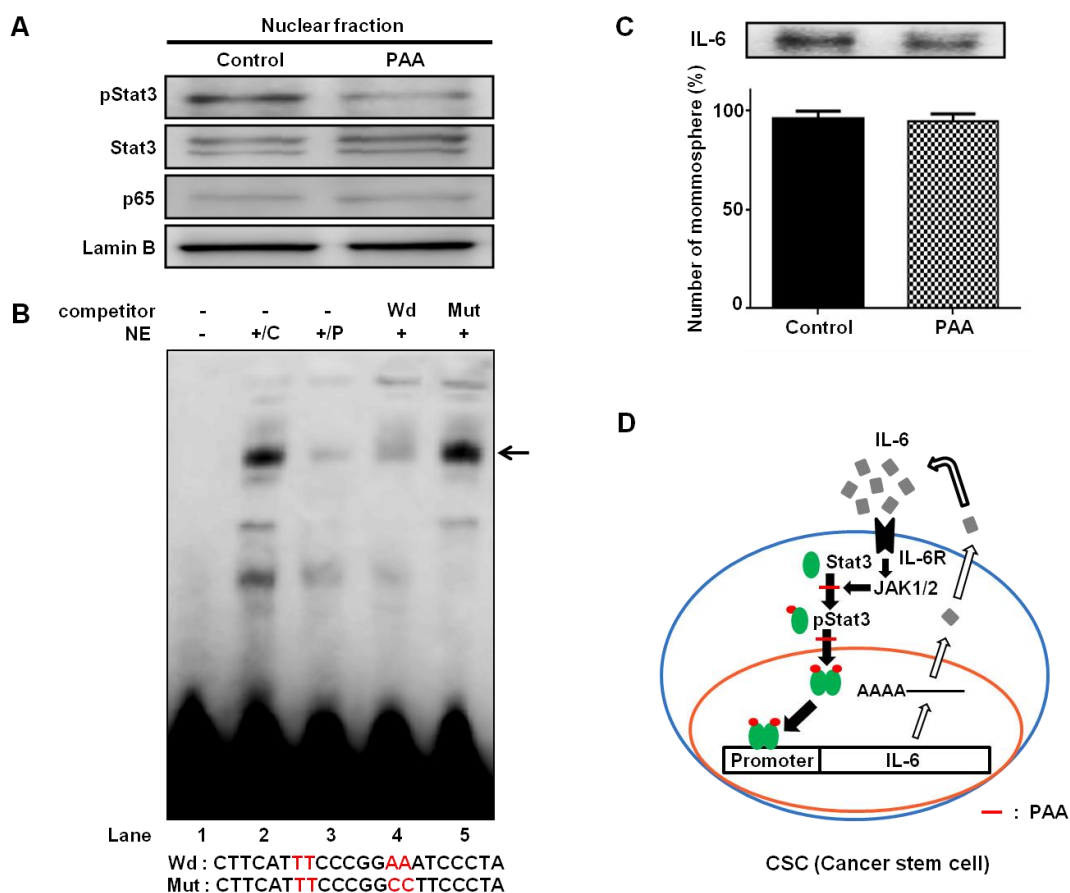


Figure 6. The effects of PAA on the Stat3 signaling pathway and IL-6 secretion in MCF-7 mammospheres. (A) The expression levels of nuclear proteins were determined by western blot with indicated antibodies. Equal protein loading was evaluated by Lamin B. (B) MCF-7 mammospheres were treated with 0.4 mM PAA for 48 h and the nuclear extracts were analyzed by EMSA. Nuclear extracts (5 μ g; NE) were incubated with biotin-labeled Stat3 probes for 20 min. Lane 1 indicates probe alone; lane 2, probe with nuclear extract; lane 3, probe with PAA-treated nuclear extract; lane 4, competition with excess unlabeled probe; lane 5, competition with unlabeled mutant probe. (C) Western blot was performed with mammosphere culture broth using an IL-6 antibody. Numbers of mammospheres with/without PAA was used as an internal control. (D) A diagram represents the model for CSCs formation mediated by Stat3 signaling pathway and IL-6. Phosphorylated Stat3 molecules form dimers, translocate into the nucleus where they bind to promoter of IL-6

gene, and activate IL-6. The secreted IL-6 regulates dynamic equilibrium between NSCCs and CSCs [26]. PAA reduced conversion of NSCCs to CSCs through dephosphorylation of Stat3 and deregulation of IL-6 secretion.

4. Discussion

The overall worldwide breast cancer is a public health problem and a leading cause of cancer death among woman. Despite improvements in detection and the diverse therapies, morbidity and mortality from breast cancer remains high because of therapy-resistant cancer cells that are responsible for disease relapse and metastasis [27]. Recent studies have shown that limited effect of breast cancer therapy is attributed to the existence of CSCs. CSCs, which compose a small fraction of the tumor bulk, show high capacities for self-renewal, tumor initiation, recurrence, metastasis and resistance to conventional therapies [28]. Therefore, elimination of CSCs is essential for treating breast cancer. In this study, we examined that PAA, a flavor and aroma volatile compound, potentially exerts activity of anti-breast CSCs in both breast cancer cell lines and mouse xenograft models.

We found that PAA significantly abrogated breast cancer cell proliferation, migration and colony formation as well as induced apoptosis (Fig. 1). In an *in vivo* mouse xenograft model, PAA suppressed tumor growth in MDA-MB-231 cells (Fig. 2). Additionally, we assessed the effect of PAA on breast CSCs through mammosphere formation assay and quantification of specific CSCs marker. In breast cancer, CD44^{high}/CD24^{low} cells and ALDH+ cells are considered to be breast CSCs [7, 29]. Our results showed that PAA inhibited the mammosphere formation of both MCF-7 and MDA-MB-231 cells (Fig. 3). PAA treatment also decreased proportion of CD44^{high}/CD24^{low} and ALDH+ breast cancer cells (Fig. 4). Moreover, PAA reduced the transcriptional levels of the CSC markers such as Nanog, Sox2, Oct4, and CD44 (Fig. 5A). These genes are established regulators and promoters of CSC phenotype. Decrease in the expression of these genes on PAA treatment indicates its potential to suppress CSC programs [30, 31]. Breast CSCs produce lower ROS levels and enhanced ROS defense than non-CSCs, which contribute to tumor radio-resistance [32, 33].

Thus, we evaluated the levels of ROS after PAA treatment and results showed that PAA induced ROS activity in MDA-MB-231 cells (Fig. 5B).

In breast CSCs, inflammatory-related signaling responses, such as nuclear factor- κ B (NF- κ B) and Stat3 have contributed to this phenotype. Recently, Stat3 activation was described as pivotal in inflammatory signaling and maintenance of breast CSCs by controlling self-renewal and differentiation. In addition, recent studies have shown that activation of NF- κ B has been related to many aspects of tumorigenesis. Hence, the Stat3 and NF- κ B pathways are promising target for cancer therapy [34, 35]. Thus, we examined the phosphorylation of Stat3 and nuclear translocation of NF- κ B after treatment PAA in breast mammospheres. Our results showed that PAA reduced nuclear translocation of phospho-Stat3 but did not reduce the nuclear p65 levels (Fig. 6A). PAA also decreased Stat3 DNA binding activity (Fig. 6B). Together, PAA reduced mammosphere formation via specifically inhibition of the Stat3 signaling pathway.

Cytokines and growth factor by activation of Stat3 promote self-renewal and help in maintaining CSCs [21, 36]. The secreted IL-6 can convert NSCCs to CSCs and regulate the dynamic equilibrium between NSCCs and CSCs. Therefore, regulation of IL-6 secretion is important for breast cancer therapy [26]. PAA inhibited production of secreted IL-6 and may be a candidate of blockade of IL-6 secretion (Fig. 6C). In conclusion, our findings are the first to provide convincing evidence that PAA inhibits breast CSCs by blocking an inflammatory pathway containing Stat3 signaling and IL-6. These findings suggest that PAA may serve as an effective agent for the treatment of breast cancer.

References

1. Ferlay J, Soerjomataram I, Dikshit R, et al. Cancer incidence and mortality worldwide: sources, methods and major patterns in GLOBOCAN 2012. *Int J Cancer*. 2015; 136:E359-E386.
2. Al-Ejeh, F. et al. Breast cancer stem cells: treatment resistance and therapeutic opportunities. *Carcinogenesis*. 2011; 32:650–658.
3. Pinto, C. A., Widodo, E., Waltham, M. & Thompson, E. W. Breast cancer stem cells and epithelial mesenchymal plasticity - Implications for chemoresistance. *Cancer Lett*. 2013; 341:56–62.
4. Reya T, Morrison SJ, Clarke MF, Weissman IL. Stem cells, cancer, and cancer stem cells. *Nature*. 2001; 414:105–111.
5. T. Lapidot, C. Sirard, J. Vormoor, B. Murdoch, T. Hoang, J. Caceres-Cortes, M. Minden, B. Paterson, M.A. Caligiuri, J.E. Dick. A cell initiating human acute myeloid leukaemia after transplantation into SCID mice. *Nature*. 1994; 367:645-648.
6. Visvader JE and Lindeman GJ. Cancer stem cells in solid tumours: accumulating evidence and unresolved questions. *Nat Rev Cancer*. 2008; 8(10):755-768.
7. Marcato P, Dean CA, Giacomantonio CA and Lee PW. Aldehyde dehydrogenase: its role as a cancer stem cell marker comes down to the specific isoform. *Cell Cycle*. 2011; 10(9):1378-1384.

8. Al-Hajj M, Wicha MS, Benito-Hernandez A, Morrison SJ and Clarke MF. Prospective identification of tumorigenic breast cancer cells. *Proc Natl Acad Sci U S A*. 2003; 100(7):3983-3988.
9. Karamboulas, C. & Ailles, L. Developmental signaling pathways in cancer stem cells of solid tumors. *Biochim. Biophys. Acta*. 2013; 1830:2481–2495.
10. Prud'homme GJ. Cancer stem cells and novel targets for antitumor strategies. *Curr Pharm Des*. 2012; 18(19):2838-2849.
11. Takebe N, Harris PJ, Warren RQ, Ivy SP. Targeting cancer stem cells by inhibiting Wnt, Notch, and Hedgehog pathways. *Nat Rev Clin Oncol*. 2011; 8:97–106.
12. Wei, W., & Lewis, M.T. Identifying and targeting tumor-initiating cells in the treatment of breast cancer. *Endocr Relat Cancer*. 2015 June; 22(3):R135–R155.
13. Fouse, S. D. & Costello, J. F. Cancer Stem Cells Activate STAT3 the EZ Way. *Cancer Cell*. 2013; 23:711–713.
14. Zhou J, Zhang H, Gu P, Bai J, Margolick JB and Zhang Y. NF-kappaB pathway inhibitors preferentially inhibit breast cancer stem-like cells. *Breast Cancer Res Treat*. 2008; 111(3):419-427.
15. Liu S, Ginestier C, Ou SJ, Clouthier SG, Patel SH, Monville F, Korkaya H, Heath A, Dutcher J, Kleer CG, Jung Y, Dontu G, Taichman R and Wicha MS. Breast cancer stem cells are regulated by mesenchymal stem cells through cytokine networks. *Cancer Res*. 2011; 71(2):614-624.

16. Kobayashi, C. I. & Suda, T. Regulation of reactive oxygen species in stem cells and cancer stem cells. *J. Cell. Physiol.* 2012; 227:421–430.
17. Chen K, Huang YH and Chen JL. Understanding and targeting cancer stem cells: therapeutic implications and challenges. *Acta Pharmacol Sin.* 2013; 34(6):732-740.
18. Buettner R, Mora LB, Jove R. Activated STAT signaling in human tumors provides novel molecular targets for therapeutic intervention. *Clin Cancer Res.* 2002; 8:945–954.
19. Diaz N, Minton S, Cox C, Bowman T, Gritsko T, Garcia R, et al. Activation of stat3 in primary tumors from high-risk breast cancer patients is associated with elevated levels of activated SRC and survivin expression. *Clin Cancer Res.* 2006; 12:20–28.
20. Sansone P, Storci G, Tavolari S, Guarnieri T, Giovannini C, Taffurelli M, et al. IL-6 triggers malignant features in mammospheres from human ductal breast carcinoma and normal mammary gland. *J Clin Invest.* 2007; 117:3988–4002.
21. Korkaya H, Liu S, Wicha MS. Breast cancer stem cells, cytokine networks, and the tumor microenvironment. *J Clin Invest.* 2011; 121(10):3804–3809.
22. Kim SY, Kang JW, Song X, Kim BK, Yoo YD, Kwon YT and Lee YJ. Role of the IL-6-JAK1-STAT3-Oct-4 pathway in the conversion of non-stem cancer cells into cancer stem-like cells. *Cell Signal.* 2013; 25(4):961-969.
23. Tieman D, Taylor M, Schauer N, Fernie AR, Hanson AD and Klee HJ. Tomato aromatic amino acid decarboxylases participate in synthesis of the flavor volatiles

- 2-phenylethanol and 2-phenylacetaldehyde. *Proc Natl Acad Sci U S A*. 2006; 103(21):8287-8292.
24. Clarke ML, Burton RL, Hill AN, Litorja M, Nahm MH and Hwang J. Low-cost, high-throughput, automated counting of bacterial colonies. *Cytometry A*. 2010; 77(8):790-797.
25. Shi X, Zhang Y, Zheng J and Pan J. Reactive oxygen species in cancer stem cells. *Antioxid Redox Signal*. 2012; 16(11):1215-1228.
26. Iliopoulos D, Hirsch HA, Wang G and Struhl K. Inducible formation of breast cancer stem cells and their dynamic equilibrium with non-stem cancer cells via IL6 secretion. *Proc Natl Acad Sci U S A*. 2011; 108(4):1397-1402.
27. Redig, A. J. & McAllister, S. S. Breast cancer as a systemic disease: a view of metastasis. *J. Intern. Med*. 2013; 274:113–126.
28. Sun X, Jiao X, Pestell TG. et al. MicroRNAs and cancer stem cells: the sword and the shield. *Oncogene*. 2014; 33:4967–4977.
29. Marotta, L. L. et al. The JAK2/STAT3 signaling pathway is required for growth of CD44(+)CD24(-) stem cell-like breast cancer cells in human tumors. *J. Clin. Invest*. 2011; 121:2723–2735.
30. Liu, A., Yu, X. & Liu, S. Pluripotency transcription factors and cancer stem cells: small genes make a big difference. *Chin. J. Cancer*. 2013; 32:483–487.

31. Lu, X., Mazur, S. J., Lin, T., Appella, E. & Xu, Y. The pluripotency factor Nanog promotes breast cancer tumorigenesis and metastasis. *Oncogene*. 2014; 33:2655–2664.
32. Phillips TM, McBride WH and Pajonk F. The response of CD24(-/low)/CD44+ breast cancer-initiating cells to radiation. *J Natl Cancer Inst*. 2006; 98(24):1777-1785.
33. Diehn M, Cho RW, Lobo NA, Kalisky T, Dorie MJ, Kulp AN, Qian D, Lam JS, Ailles LE, Wong M, Joshua B, Kaplan MJ, Wapnir I, Dirbas FM, Somlo G, Garberoglio C, et al. Association of reactive oxygen species levels and radioresistance in cancer stem cells. *Nature*. 2009; 458(7239):780-783.
34. Pires BR, DE Amorim ÍS, Souza LD, Rodrigues JA, Mencialha AL. Targeting Cellular Signaling Pathways in Breast Cancer Stem Cells and its Implication for Cancer Treatment. *Anticancer Res*. 2016 Nov; 36(11):5681-5691.
35. Karin M: Nuclear factor-kappaB in cancer development and progression. *Nature*. 2006; 441:431-436.
36. Zhao D, Pan C, Sun J, Gilbert C, Drews-Elger K, Azzam DJ, et al. VEGF drives cancer-initiating stem cells through VEGFR-2/Stat3 signaling to upregulate Myc and Sox2. *Oncogene*. 2015 Jun 11; 34(24):3107-3119.